Available online at www.sciencedirect.com

jmr&t Journal of Materials Research and Technology

journal homepage: www.elsevier.com/locate/jmrt

Effect of agar concentration on structure and physiology of fungal hyphal systems

Elise C. Hotz [a], *Alexander J. Bradshaw* [b], *Casey Elliott* [c], *Krista Carlson* [c], *Bryn T.M. Dentinger* [b], *Steven E. Naleway* [a,*]

[a] *The University of Utah Department of Mechanical Engineering, USA*
[b] *Natural History Museum of Utah & School of Biological Sciences, University of Utah, USA*
[c] *The University of Nevada-Reno Department of Materials Science and Engineering, USA*

ARTICLE INFO

Article history:
Received 4 April 2023
Accepted 2 May 2023
Available online 5 May 2023

Keywords:
Fungi
Permeability
Hyphae
Material science

ABSTRACT

Hyphae are the filamentous branches that form a mycelial network, acting as the constitutive structure of mushroom-forming *Fungi*. Hyphae grow on many substrates and in multitudes of environmental conditions. Due to this versatility, hyphae are of increasing interest in the area of bio-constructed materials derived from sustainable and non-petroleum-based inputs. By understanding the effects of external factors on the growth and physical properties of the hyphae, we can manipulate the physical properties of a cultivated mycelial sheet. This study demonstrates how altering the agar concentration during *in vitro* culturing can affect the physical growth and structure of the mycelial sheet without altering its permeability or chemical makeup. When the agar concentration was increased from 1.5% agar to 6.0% agar, the mycelium density and hyphal width increased by 32.3% and 63.6%, respectively. The implications of these findings will allow for the advancement and tuning of fungi-based materials, particularly for the application of sustainable textiles and fine particulate filters.

1. Introduction

Fungi is a highly diverse section of life, with a prolific distribution found in nearly every biome investigated on Earth [1]. *Fungi* have developed numerous adaptions to grow and thrive under the most extreme environmental conditions [2]. This range of environmental stressors has allowed for some species of *Fungi* to develop unique adaptions in order to survive. For example, researchers have found some fungal structures to possess fire-retardant and antibacterial properties [3]. Furthermore, *Fungi* can be fast-growing, are considered carbon negative due to their role in sequestering carbon in the soil, and can thrive on a wide variety of substrates from wood to jet fuel [4–8]. The breadth of these physical adaptions has fueled growing interest in how engineers can manipulate fungal microstructures for practical applications, such as biocomposites, building materials, and textiles [9]. As a result, *Fungi* are being studied as a promising sustainable alternative for everything from plastics and foams to leather and textiles [10]. A deeper understanding of the factors which influence *Fungi's* microstructure will allow further exploration into their potential uses as a biomaterial.

The key to *Fungi's* malleable microstructure is in the hyphae. Hyphae are filamentous branches of fungal cells with

* Corresponding author.
E-mail address: steven.naleway@mech.utah.edu (S.E. Naleway).
https://doi.org/10.1016/j.jmrt.2023.05.013

chitinous cell walls. They serve the purpose of extracting nutrients from the biological substrates and are capable of growing through biological material (e.g., lignin, cellulose, and detritus) [11–13]. As hyphae proliferate, they form a complex vegetative network called mycelium (Fig. 1). The properties of the mycelial network are biologically plastic and can be manipulated by changing or altering the substrate on which they are grown [10]. Common species of *Fungi* such as *Ganoderma lucidum* and *Pleurotus ostreatus* can be propagated with a simple solution of cellulose and potato dextrose, and were shown to grow longer, thinner, and more elastic hyphae compared to those grown on a complex cellulose substrate [10]. The ability to directly influence the microstructure of mycelium allows for unique applications such as targeted fine particulate filtration. To illustrate this potential, mycelium composites have already successfully filtered fine particulate matter such as Nitrate and Sulphate, harvested water from fog, and remediated soil contaminated by heavy metals [14–16]. Through the alteration of media on which a mycelial mat is grown, it becomes possible to influence the mycelial sheet's physical structure for desired material properties [10].

Despite the growing interest in *Fungi* and their potential uses as biomaterials, details on the physical factors that affect hyphal growth and the resulting structure of the mycelial sheet are heavily understudied. Current research is limited to looking at how manipulations of the growth environment's physical properties may impact the fungal mycelium's microstructure. In particular, it is unclear how the density of the substrate, one of the easiest to manipulate variables in the culturing of *Fungi*, affects growth patterns and the physical properties of a mycelial sheet. Studying how the substrate affects hyphal growth patterns, such as the width of the hyphal cells and the density of the mycelium network, will help develop fungal derived biomaterials, such as textiles and filters.

This study uses SEM imaging, permeability testing, and chemical characterization to observe the relationship between agar concentration and hyphal growth. *Pleurotus populinus* is commonly used in materials applications due to its ability to grow in a variety of environmental conditions. *P. populinus* is also fast growing and ideal for potential scale-up in industry applications [17,18]. *P. populinus* was cultured on agar plates of four concentrations: 1.5%, 3.0%, 4.5%, and 6.0%. The resulting microstructure was analyzed for mycelium density, hyphal width and pore diameter. The permeability was recorded and compared to other porous filter materials. The chemical composition of the mycelium grown under each condition was also analyzed using Fourier-transformed infrared spectroscopy (FTIR) to ensure that all samples received the same nutrients throughout the growth period. The ability to alter the microstructure of the mycelium without changes to the chemical composition will allow for the creation of more sustainable filtration membranes that are able to target specific sizes of particulate matter.

2. Materials and methods

2.1. Preparation of substrates

Growth media for fungal cultures was made using 2% (20 g/L) malt extract (Fisher Scientific cat no: ICN15531590) and increasing concentrations of agar, 1.5%(15 g/L), 3%(30 g/L), 4.5%(45 g/L), and 6%(60 g/L) (ThermoFisher cat no: AC443572500). Growth media was autoclaved for 30 min at 121 °C on a liquid cycle and allowed to cool to ~60 °C to allow for the addition of antibiotic ampicillin at a final concentration of 50 μg/ml to stave off any bacterial contamination. Forty-five plates of each density agar were poured, resulting in a total of 180 plates. Cellophane of 2.8-mm thickness was cut into 70 cm squares and autoclaved for 20 min at 121 °C. Each plate was labeled in a laminar fume hood, and a cellophane square was placed on the substrate surface to make the removal of mycelium after culturing possible for processing. The bulk density of the agar was measured by cutting out two agar cubes of 1 cm^3 from three plates of each concentration for a

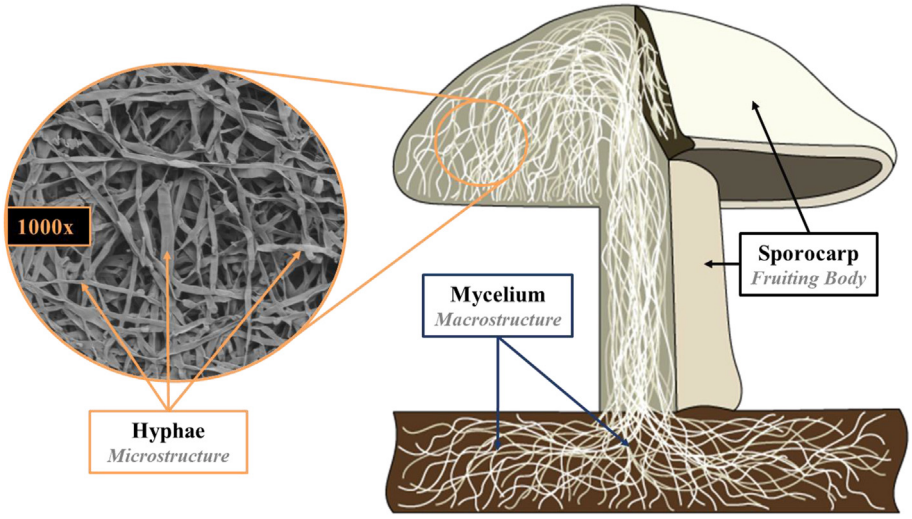

Fig. 1 – Diagram of the cross-section of a mushroom sporocarp, showing the mycelium macrostructure and the hyphal microstructure.

total of 24 cubes (six for each concentration). The cubes' volume (cm^3) and mass (g) were recorded and used to calculate the average density over each agar concentration.

2.2. Culturing and growth of mycelia sheets

Specimens of *P. populinus* were sub-cultured from sterile tissue of wildly collected sporocarps that are actively maintained by the Dentinger research group at the University of Utah. Isolated sections of contiguous mycelium from initial spore plates were subcultured by removing ~2 cm^2 of tissue from the edge of the growing mycelium with a flame-sterilized scalpel and seeded onto the previously prepared plates. The inoculated plates were sealed with Parafilm and stored in low light conditions at 20 °C. The samples were allowed to propagate for six weeks to ensure that the mycelium was robust enough for handling and imaging.

2.3. Microstructure characterization

Structural characterization was accomplished via imaging of the mycelial mats. The plates were heat treated for 1 h at 68 °C to desiccate the samples. Imaging specimens were cut from the plates after heat treatment. Four plates from each agar density were used, and one specimen was cut from each plate resulting in 16 total specimens, four from each density. Specimens were coated with 20 nm of gold-palladium to reduce electron charging. The specimens were imaged using an FEI Quanta 600FE-ESEM scanning electron microscope (Quanta, Hillsboro, OR, USA) at an accelerating voltage of 5 kV to mitigate overcharging the samples and a spot size of 5 nm. Five images at 1000x magnification were taken at dispersed locations on each specimen resulting in 80 images total. These eighty images were analyzed using Image-J to determine hyphal width, mycelium density, and pore diameter. The mycelium density was measured as the percent of the area occupied by hyphae versus the total area of the image, resulting in 80 total mycelium density measurements, 20 for each agar density. Hyphal width was evaluated by measuring the approximate width of the hyphae. Five hyphal width measurements were taken from each image resulting in 400 total measurements, 100 for each agar density. The pore diameter, or space between the hyphae, was approximated by the DiameterJ plug-in. The pore diameter was approximated using the average of 20 pore measurements from each image, 1600 total measurements.

2.4. Growth rate

Three plates of the four-agar densities (12 plates total) were cultured with a mycelium plug of *P. populinus* and observed over 15 days. From the time of culturing, images of each plate were taken every 24 h for 15 days to document the growth patterns of the mycelium on each substrate. A total of 180 images were taken, one image per plate per day. These images were then analyzed using image-J software by measuring the diameter of the mycelium on the plate. Due to the irregular radial growth pattern of the hyphae, three diameter measurements were averaged for each image resulting in 45 total measurements for each plate. OriginPro® was used to create a linear model to approximate the average growth rate for each density.

2.5. Permeability

The permeability was measured to study the efficacy of mycelium as a sustainable replacement material for fine particulate filters. Three samples for each agar concentration were tested at three flow rates within the linear regime (1 standard cubic centimeter per second by volume (sccsv), 2 sccsv, 3 sccsv). The permeability values were averaged for each sample at the given flow rates and between the three samples of the corresponding agar concentrations. Helium permeabilities of mycelium samples were measured through steady-state gas flow measurements using a custom-designed flow setup (Fig. 2). Polydimethylsiloxane (PDMS) holders were set for 24hrs in 3D-printed molds designed to mold the holders to provide an airtight seal for mycelium samples. The PDMS holders and sample were inserted into an airtight glass tube and connected in line with the helium supply. A working flow range of helium (1–3 sccsv) was controlled using an Omega FMA-2618A mass flow controller (0.8% accuracy, Omega Engineering, Norwalk, CT, USA) and an Omega FMA-2617A mass flow meter (0.8% accuracy, Omega Engineering, Norwalk, CT, USA) was used to observe and calculate the resulting pressure drop. Once a linear regime was established, Darcy's law of fluid flow (Eq. (1)) through a porous medium was applied flow rates within the linear working range, to calculate permeability:

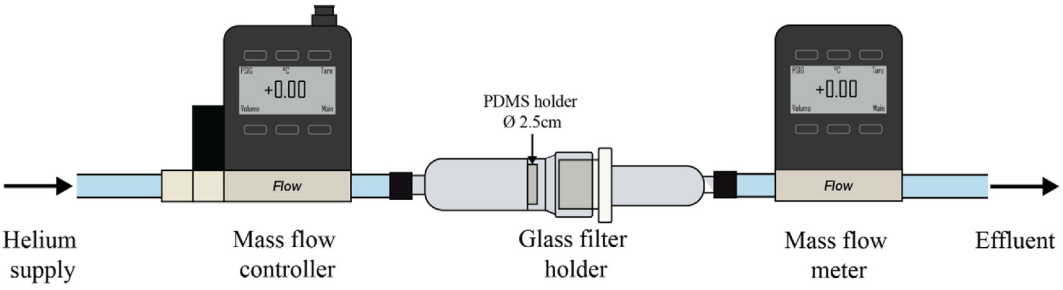

Fig. 2 – The flow setup for permeability testing. A test apparatus consisting of a helium supply, a digital mass flow controller used to regulate the face velocity of the gas, a glass filter holder containing a PDMS holder, and a digital mass flow meter used to record the effluent flow and pressure from the samples. The glass filter holder is 15 cm in length. Inspired by [19].

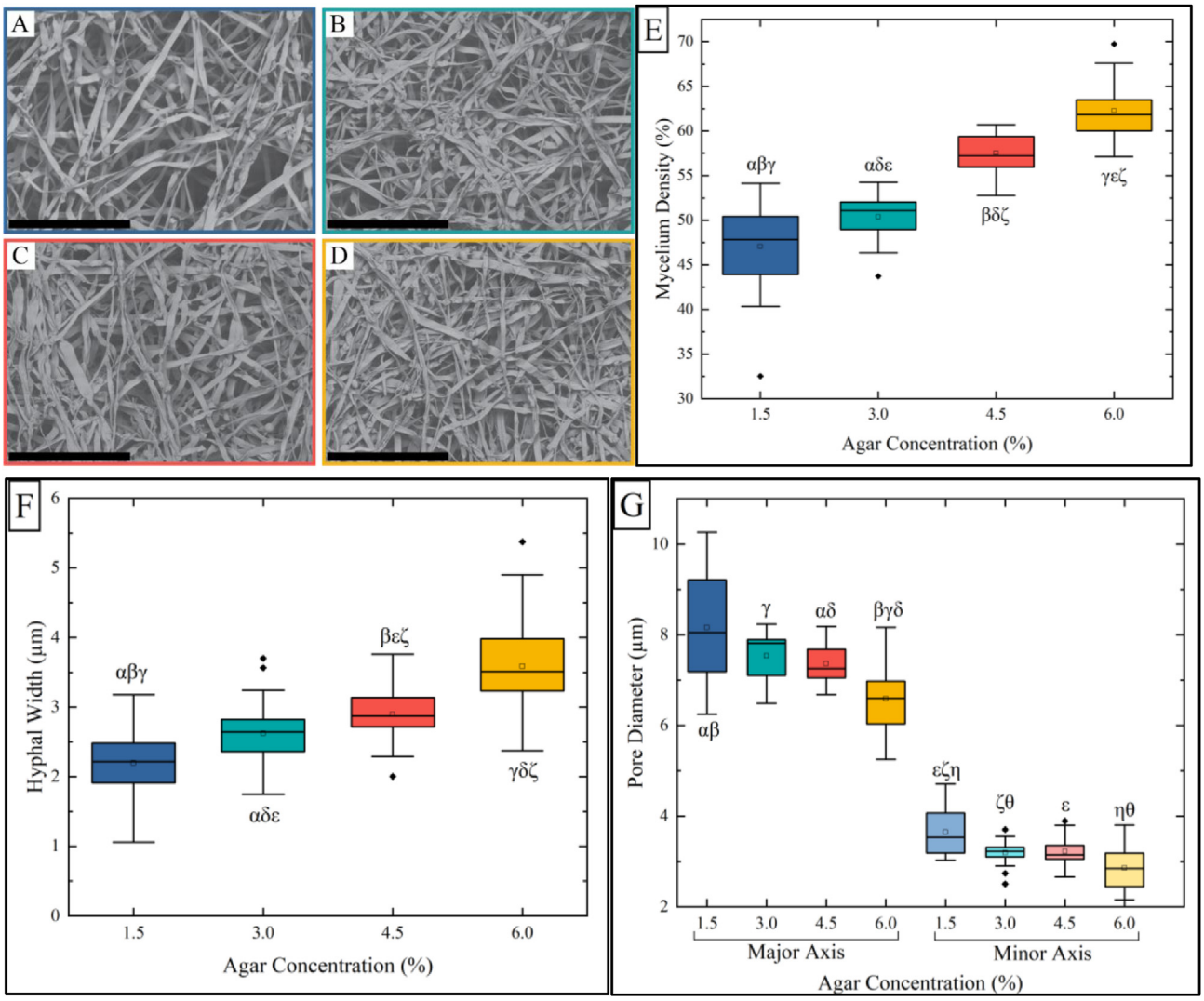

Fig. 3 – Representative SEM images of the hyphal structure showing the increase in hyphal density (%) and hyphal width (μm) and decreasing pore diameter (μm) with increasing agar concentration with images for (A) 1.5% agar density, (B) 3.0% agar density, (C) 4.5% agar density, and (D) 6.0% agar density. (E) Box plot of mycelium density vs. agar concentration. Data are presented as the average of N = 20 for each box. (F) Boxplot of hyphal width vs. agar concentration. Data are presented as the average of N = 100 for each box. (G) Box plot of pore diameter (μm) showing the averages for the major and minor axis of the elliptical approximations vs. agar concentration. Data are presented as the average of N = 20 for each box. Matching Greek letters above or below boxplots indicates a statistically significant difference at a significance level of α = .05. The scale bars indicate 50 μm.

$$K = \frac{Q^{*}\eta^{*}L}{\Delta P^{*}A} \quad (1)$$

where the length of the porous medium, L (cm), the pressure drop, ΔP (g cm^{-1} s^{-2}), the volumetric flow rate, Q (cm s^{-1}), the fluid viscosity, η (g cm^{-1}s^{-1}), and the cross-sectional area, A (cm^2) were used to calculate the permeability, K (cm^2), which was converted into units of m^2 for final reporting. Previous work has shown this process to successfully measure the permeability of other biological tissue, including live celery plants [19]. In addition to the mycelium, the permeability of various comparable particulate filters were measured, including; borosilicate glass, a grade A quartz microfiber (QMA) filter, a surgical mask, an N95 mask, and paper.

2.6. *Chemical characterization*

The chemical compositions of mycelium grown on the four agar densities were compared using Fourier-transformed infrared spectroscopy (FTIR). One FTIR sample was used for mycelium from each growing condition, resulting in four total spectra. FTIR spectra were collected for each of the four agar concentrations, 1.5%, 3.0%, 4.5%, and 6.0% using a Thermo Scientific Nicolet 380 equipped with OMNIC software (Thermo Fisher Scientific, Waltham, MA, USA). Spectrum collection was completed by placing the FTIR samples onto a clean, diamond-tipped attenuated total reflection window and compressing them via a pressure tower. The scan range for all four samples was 900–4000 cm^{-1}, and all measurements were

recorded at ambient conditions. This analysis was used to control for nutrient uptake by the hyphae to ensure that the chemical composition was not affected by the change in agar concentration.

2.7. Statistical analysis

Statistical analyses were performed using R Studio and OriginPro®. Statistical significance was determined using a One-way ANOVA followed by a Tukey's HSD post-hoc test at a significance level of $\alpha = .05$. Statistical significance was assessed for hyphal density, hyphal width, growth rate, chemical composition, and permeability as a function of agar density.

3. Results and discussion

3.1. Microstructure characterization

The density of the mycelium as a function of agar density is shown in Fig. 3E. The data show that the mycelium density increased with increasing agar density. The 6% agar had the highest density at 62.2%, while the 1.5% agar had the lowest density at 47.1%. This change in hyphal density can be seen in the images shown in Fig. 3A–D. These images show that as the agar concentration increases, the hyphae grow closer together, creating a thicker mycelial mat. The ANOVA showed a statistically significant difference in mycelium density ($p < .001$). Fig. 3E shows that a Tukey's HSD test demonstrated a statistically significant change ($p \leq .022$) between all treatment conditions and a positive correlation between agar concentration and mycelium density.

The 6% agar also has the highest average hyphal width at 3.6 μm, and the 1.5% agar had the lowest average hyphal width at 2.2 μm. The ANOVA showed a statistically significant difference in the hyphal width ($p < .001$). As shown in Fig. 3F, Tukey's HSD tests demonstrated a statistically significant change ($p < .001$) between all treatment conditions. The data demonstrated a positive correlation between agar concentration and hyphal width.

Fig. 3G shows the change in pore diameter as a function of agar concentration. The 6% agar has the lowest average pore diameter based on an elliptical approximation, with major and minor axis at 6.7 μm and 2.9 μm. The 1.5% agar had the highest average pore diameter, with major and minor axis averaging 8.2 μm and 3.7 μm. The ANOVA showed a statistically significant difference in the pore diameter ($p < .001$). As shown in Fig. 3G, a Tukey's HSD test demonstrates a statistically significant change for the pair-wise comparison between the mycelium grown on the 1.5% and 6.0% agar for the major and minor axis of the elliptical approximation ($p < .001$). The data demonstrated a negative correlation between agar concentration and hyphal pore diameter.

Previous research has studied mycelial growth through the soil in three dimensions. The density of mycelium has been shown to be affected by the bulk density of soil. As the bulk density of the soil increases, there is a decrease in the net pore volume of the mycelium [20]. Increasing the bulk density of the soil has also been shown to increase the colonization rate (i.e., spore distribution) in species of *Rhizoctonia solani* [21]. Smaller pores in the mycelial sheet were also found to be a function of increasing the bulk density of the soil. The increase in mycelium colonization and the smaller pores are attributed to increased substrate continuity at higher bulk densities. These findings support the results observed when growing mycelium on an agar substrate in two dimensions. As shown in Table 1, the bulk density of agar increases with agar concentration, enabling the mycelium to form a tighter hyphal network and smaller pores. Similarly, the bulk density of soil ranges from 0.2 g/cm^3 for peat to 2.0 g/cm^3 for glacial till [22]. The 3.0% agar is similar to that of silt loam at 1.5 g/cm^3, while the 6.0% has a bulk density just over that of glacial till.

3.2. Growth rate

Fig. 4A shows that over 15 days, the mycelium grown on the 6.0% agar grew faster in the radial direction than the mycelium grown on the 1.5% agar. Fig. 4B shows the variance in growth rate between the high and low-density samples as well as the average growth plotted over time for all four agar densities. At the end of the 15-day growth period, the 6% agar had filled out the culturing plate (10 cm diameter), where the 1.5% agar had shown the slowest growth. The approximate growth rates for 6% and 1.5% agar are modeled by linear equations resulting in average growth rates of 0.79 cm/day and 0.64 cm/day with R^2 values of 0.995 and 0.993, respectively. Previous works cite mycelium growing 0.6–0.8 cm/day and as high as 1–1.2 cm/day [23–25]. Fungal mycelium grows faster than most species of wood used in consumer products, requires few resources such as large amounts of land or water, and can grow on nutrients of decomposing waste material [26–29]. Furthermore, cattle used for leather production take at least two years to mature, while mycelium mats are grown in weeks [26,30]. Leather properties can also vary based on the age and environmental conditions of the cattle, and the hides are unusable if they have too many imperfections from injury or parasites [30,31]. Controlling the growth rate of mycelium could improve production efficiency by producing material in higher volumes, with fewer resources, than traditional materials such as wood and leather.

3.3. Permeability

Table 2 shows the measured permeability and approximate pore diameter of mycelium and a variety of filters, including borosilicate glass, QMA glass, a surgical mask, an N95 mask, and paper for comparison. The mycelium samples all demonstrated permeability values on the order of 10^{-13} m^2.

Table 1 – Density (g/cm^3) of substrate for each agar percentage. Data are presented as the average of N = 6.

Agar Percent (%)	Average Density (g/cm^3)
1.5	0.97
3.0	1.47
4.5	2.09
6.0	2.17

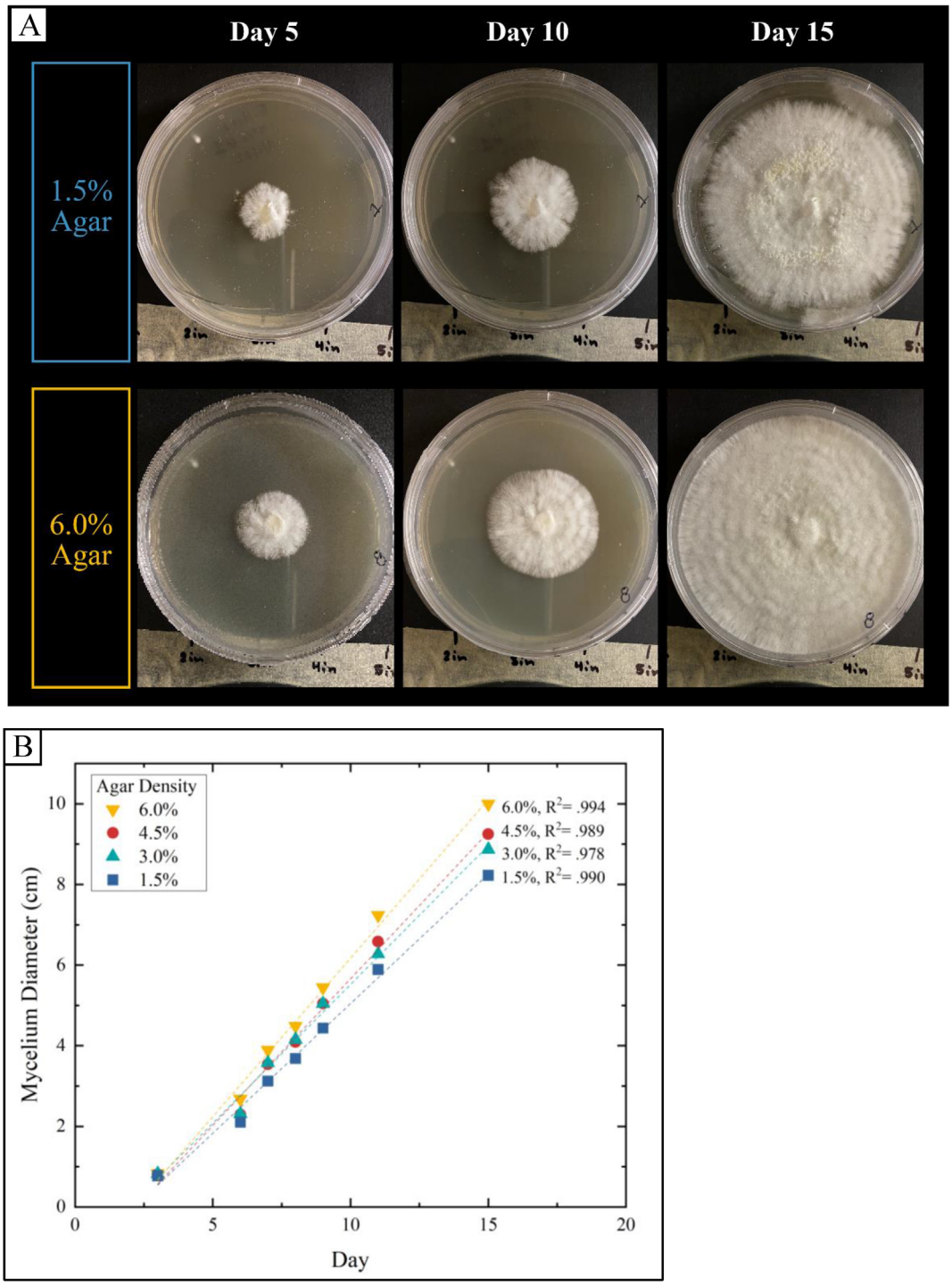

Fig. 4 – Growth rate images and data for the mycelium samples over 15 days. (A) Mycelium growth rate at days 5, 10, and 15 for 1.5% and 6.0% agar concentrations. (B) Growth trends for mycelium samples grown on substrates of 1.5%, 3.0%, 4.5%, and 6.0% agar concentration. Linear trend lines and R^2 values are included for all samples. Data are presented as the average of N = 4 at each data point.

Statistical analysis using one-way ANOVA showed no statistical difference between the permeability values of different agar concentrations ($p = .0534$). The change in permeability between the mycelium samples was within the standard error of the equipment and there was no statistically significant change, despite statistically significant changes in mycelium density, hyphal width, and pore diameter. Factors not accounted for in the Darcy equation include void ratio (mycelium density), pore diameter, and cross-sectional structure of the material. While the mycelium density and pore diameter were statistically significant, they did not affect the permeability of the sample in a significant way.

Table 2 – Helium permeability with standard deviation and pore diameter for mycelium (1.5%), mycelium (6.0%), boro glass filter, QMA filter, reusable and single-use surgical masks, an N95 mask, and printer paper. Permeability data are presented as the average and standard deviation of N = 9. Data for mycelium is presented as major and minor axes of an elliptical approximation. Data for all other materials are presented as an average pore diameter. Pore diameter data is presented as the average of N = 400. *Pore diameter data adapted from [38,39].

Material	He Permeability k (m^2x10^{-13})	Standard Deviation (m^2x10^{-13})	Pore Diameter (μm)
Mycelium (1.5% Agar)	5	0.82	8.2, 3.6
Mycelium (6.0% Agar)	5.5	0.74	6.5, 2.9
Boro Glass Filter	3	0.3	3.1
QMA Glass Filter	7	0.8	2.2
Reusable Mask	4	NA	47*
Single-use surgical mask	5	1	33*
N95 mask	30	4	30*
Printer paper	0.1	0.001	12

This finding can be applied to the development of permeable membranes and filters. The pore diameter can be changed to trap different-sized particles while maintaining a similar degree of airflow through the material. In addition to the mycelium samples, various filters were tested for permeability and pore diameter (Table 2). The mycelium was shown to have a permeability similar to that of a surgical mask. The mycelium grown on the 1.5% agar had a pore diameter within 15 μm of the surgical mask pores. The mycelium grown on the 6% agar has a pore diameter similar to that of paper. Previous studies have demonstrated fungal chitin's efficacy in synthesizing nanopaper filters [32]. Such filters successfully blocked 10 nm gold nanoparticles, a metric that may indicate the potential for the filtration of viruses. The smallest respiratory droplet able to carry SARS-CoV-2 is estimated to be 9.3 μm; this is larger than the average pore diameter of the 1.5% agar concentration mycelium and larger than the maximum pore measurement from the 6% agar concentration mycelium [33]. This pore diameter also falls below the commonly measured PM10 (particulate matter less than or equal to 10 μm) [34]. PM10 is a common public health concern for people in urban areas and has many sources, including automobile pollution, construction debris, and environmental dust [35–37]. Mycelium-based filters could help create more sustainable options for air filtration and face coverings used to protect people from PM10.

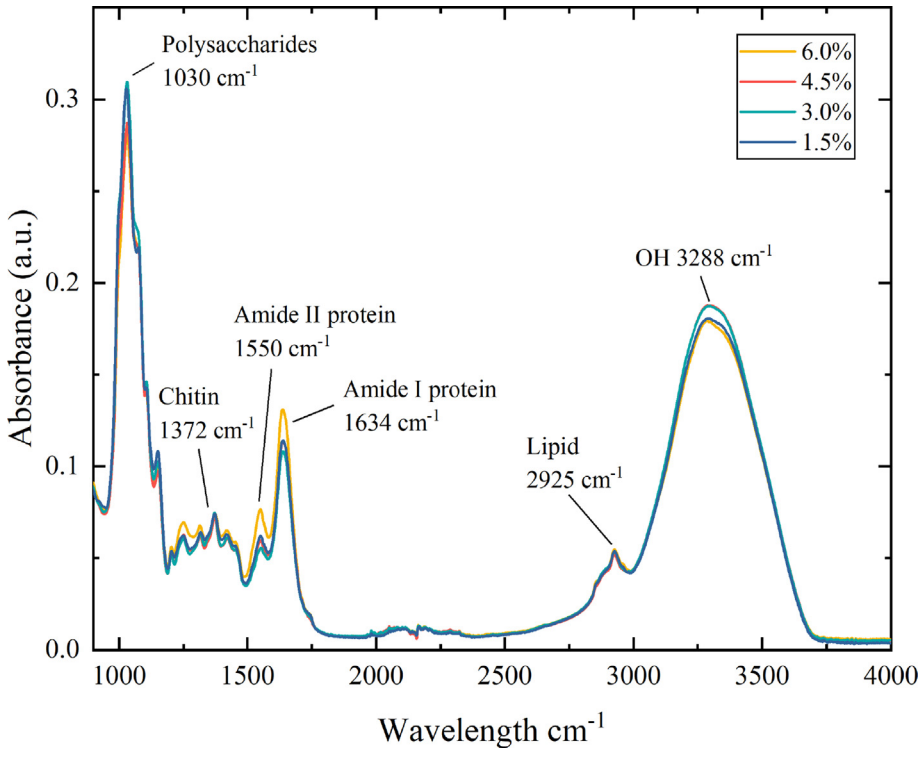

Fig. 5 – Data from the Fourier transform infrared (FTIR) spectra for the mycelium samples grown on substrates of 1.5%, 3.0%, 4.5%, and 6.0% agar concentration. Agar density does not have a significant effect on the chemical composition of the hyphae. Data are presented as the average of N = 2 at each data point.

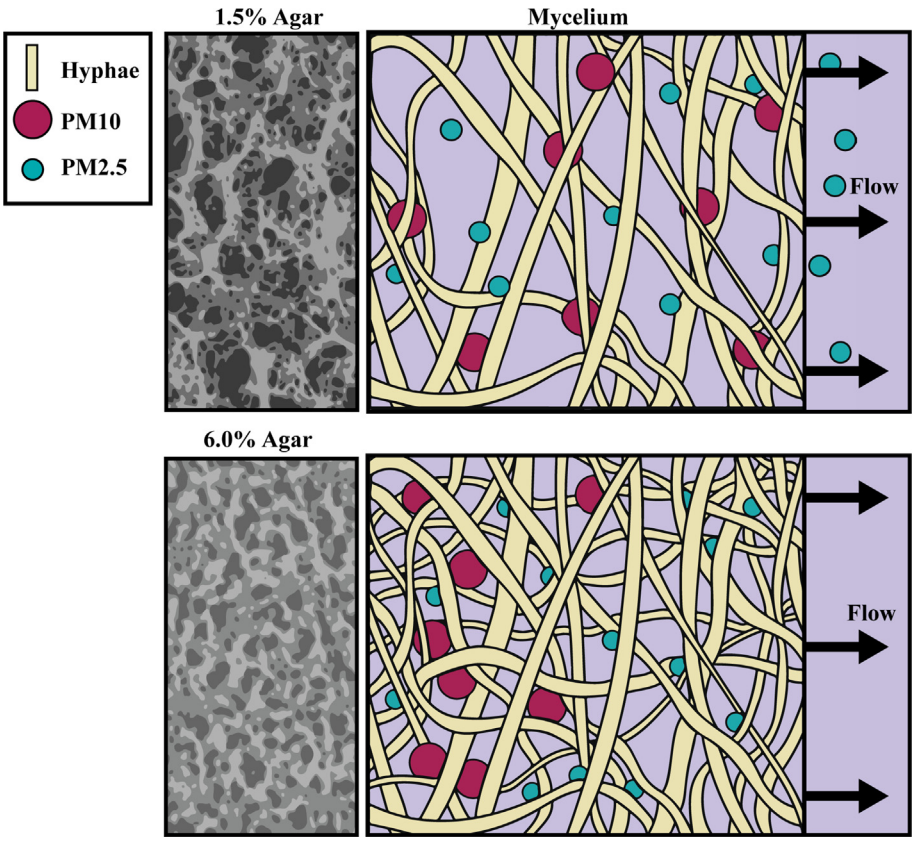

Fig. 6 – Demonstration of the effect of changing agar density on the physiological development of the mycelial sheet and how this can be used to trap particulate matter of varying sizes. The 1.5% agar produces a more open structure in the mycelial sheet, while the 6.0% agar causes the mycelium to form a denser network.

3.4. *Chemical characterization*

FTIR was used to study the chemical composition of each agar density. Fig. 5 shows the absorbance spectra of the hyphae samples. The small discrepancies in lipid and amide protein concentrations with differences less than 10% ± 2% and were within the chemical variance of the samples and repeatability of the FTIR test. This shows that while the physical structure of the mycelium can be tuned to meet desired properties, the chemical composition remains uncompromised. All samples were able to uptake a similar amount of nutrients from the substrate and formed protein, fat, sugar, and chitin that varied little within the samples or between samples.

Changing the mycelial density via changes to the agar concentration can create high volumes of material in a short period of time when compared to the time required to grow

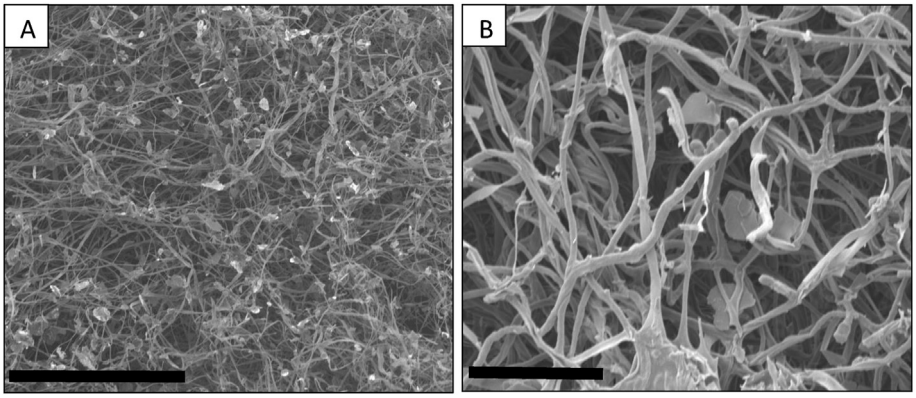

Fig. 7 – SEM imaging of 5 μm alumina platelets embeded in the mycelial network. Image A is taken at 500x magnification and the scale bar indicates 100 μm. Image B is taken at 2000x magnification and the scale bar indicates 20 μm.

other materials such as leather and wood. FTIR and permeability testing were used to show that the resulting mycelial sheets are chemically similar and have the same permeability profile. Furthermore, the permeabilities of the mycelial sheets are comparable to the values obtained for filters such as surgical masks. SEM imaging and data analysis showed a statistically significant change to the mycelium density, hyphal width, and pore diameter. The resulting mycelial sheets can be used to produce filters for different size particles through the relatively simple method of changing agar concentration. Fig. 6 shows how the 6% agar has a smaller pore size that may be better suited for filtering out small particulate matter such as PM2.5 (particulate matter less than or equal to 2.5 μm), while the 1.5% agar may be better for PM10 (particulate matter less than or equal to 10 μm), or virus particulate around 9 μm. Fig. 7 uses SEM imaging to show 5 μm alumina platelets embedded within the mycelial network. These images demonstrate the ability of mycelium to trap particulate matter and establish the potential for using mycelium in particulate filtration applications.

4. Conclusions

This study utilized imaging, permeability testing, and chemical analysis to characterize the effects of agar concentration on the growth and microstructure of a fungal hyphal system. Using these processes, the observed results lead to the following conclusions.

- Increasing the agar concentration increases the density of the mycelium as well as the thickness of the individual hyphae. This can be applied to material development applications requiring a desired microstructure, such as filtration and textile development.
- Increasing the mycelium density results in smaller pores between the hyphae. This demonstrates the potential for tuning properties, such as pore diameter, to achieve a desired filter size for varying ranges of particulate matter.
- Mycelium growth was correlated to the agar concentration with a growth rate of 0.64 cm/day at 1.5% and 0.79 cm/day at 6.0%. Mycelium is fast growing, making it an excellent option for scaling up in industry applications. The ability to control the growth rate could also be useful in batch propagation for materials of specific sizes and specifications that must be harvested on a manufacturing schedule.
- The permeability was constant, and 1.5% showed a pore diameter similar to printer paper, while 6% showed a pore diameter similar to a borosilicate filter. The permeability was recorded and compared to permeabilities of other porous filter materials, including borosilicate filters, QMA filters, reusable, surgical, and N95 masks. The results showed a statistically significant increase in the hyphal width and mycelium density when the agar concentration was increased from 1.5% to 6.0%. This change occurred without a statistically significant change to the chemical composition of the samples. Creating a denser mycelial mat without changes to permeability or material chemistry will allow for the development of new, more sustainable filter materials.

Declaration of Competing Interest

The authors declare that they have no known competing financial interests or personal relationships that could have appeared to influence the work reported in this paper.

Acknowledgements

This work was funded in part by an American Chemical Society PRF grant #65985-ND10.

REFERENCES

[1] Dix NJ, Webster J. Fungi of extreme environments. In: Dix NJ, Webster J, editors. Fungal Ecology. Dordrecht: Springer Netherlands; 1995. p. 322–40. https://doi.org/10.1007/978-94-011-0693-1_12.
[2] Zhang X, Li S-J, Li J-J, Liang Z-Z, Zhao C-Q. Novel natural products from Extremophilic fungi. Mar Drugs Jun. 2018;16(6). https://doi.org/10.3390/md16060194. Art. no. 6.
[3] Jones M, Bhat T, Kandare E, Thomas A, Joseph P, Dekiwadia C, et al. Thermal degradation and fire properties of fungal mycelium and mycelium - biomass composite materials. Sci Rep Dec. 2018;8(1). https://doi.org/10.1038/s41598-018-36032-9. Art. no. 1.
[4] Lew RR. How does a hypha grow? The biophysics of pressurized growth in fungi. Nat Rev Microbiol Jul. 2011;9(7). https://doi.org/10.1038/nrmicro2591. Art. no. 7.
[5] Raimbault M, Alazard D. Culture method to study fungal growth in solid fermentation. European J. Appl. Microbiol. Biotechnol. Sep. 1980;9(3):199–209. https://doi.org/10.1007/BF00504486.
[6] Fungo B, Buyinza J, Sekatuba J, Nansereko S, Ongodia G, Kwaga P, et al. Forage biomass and soil aggregate carbon under fodder banks with contrasting management regimes. Agroforest Syst Jun. 2020;94(3):1023–35. https://doi.org/10.1007/s10457-019-00473-6.
[7] Edmonds P, Cooney JJ. Identification of Microorganisms Isolated from jet fuel systems. Appl Microbiol Mar. 1967;15(2):411–6. https://doi.org/10.1128/am.15.2.411-416.1967.
[8] Radwan O, Gunasekera TS, Ruiz ON. Draft Genome sequence of Fusarium fujikuroi, a fungus adapted to the fuel environment. Genome Announc Jan. 2018;6(3):e01499-17. https://doi.org/10.1128/genomeA.01499-17.
[9] "A review of the material and mechanical properties of select Ganoderma fungi structures as a source for bioinspiration," springerprofessional.de. https://www.springerprofessional.de/en/a-review-of-the-material-and-mechanical-properties-of-select-gan/23986612 (accessed Mar. 14, 2023).
[10] Haneef M, Ceseracciu L, Canale C, Bayer IS, Heredia-Guerrero JA, Athanassiou A. Advanced materials from fungal mycelium: Fabrication and tuning of physical properties. Sci Rep Mar. 2017;7(1):41292. https://doi.org/10.1038/srep41292.
[11] Porter DL, Naleway SE. Hyphal systems and their effect on the mechanical properties of fungal sporocarps. Acta Biomater Jun. 2022;145:272–82. https://doi.org/10.1016/j.actbio.2022.04.011.
[12] Tuor U, Winterhalter K, Fiechter A. Enzymes of white-rot fungi involved in lignin degradation and ecological determinants for wood decay. J Biotechnol Jul.

1995;41(1):1–17. https://doi.org/10.1016/0168-1656(95)00042-O.
[13] Baldrian P, Valášková V. Degradation of cellulose by basidiomycetous fungi. FEMS (Fed Eur Microbiol Soc) Microbiol Rev May 2008;32(3):501–21. https://doi.org/10.1111/j.1574-6976.2008.00106.x.
[14] Lee T, Choi J. Mycelium-composite panels for atmospheric particulate matter adsorption. Results in Materials Sep. 2021;11:100208. https://doi.org/10.1016/j.rinma.2021.100208.
[15] Zhang Y, Zhu C, Shi J, Yamanaka S, Morikawa H. Bioinspired composite materials used for efficient fog harvesting with structures that consist of fungi-Mycelia networks. ACS Sustainable Chem Eng Sep. 2022;10(38):12529–39. https://doi.org/10.1021/acssuschemeng.2c01816.
[16] Wales DS, Sagar BF. Recovery of metal ions by microfungal filters. Journal of Chemical Technology & Biotechnology 1990;49(4):345–55. https://doi.org/10.1002/jctb.280490407.
[17] Yaeger W, Jawed M, Tauman D, Ho P, Ali A, Gomanie NN, et al. "Modular methods for oyster mushroom cultivation in low-resource settings," in 2022 IEEE. GlobalHumanitarian Technology Conference (GHTC) Sep. 2022:30–7. https://doi.org/10.1109/GHTC55712.2022.9911008.
[18] Wan Mahari WA, Peng W, Nam WL, Yang H, Lee XY, Lee YK, et al. A review on valorization of oyster mushroom and waste generated in the mushroom cultivation industry. J Hazard Mater Dec. 2020;400:123156. https://doi.org/10.1016/j.jhazmat.2020.123156.
[19] Mroz M, Ali M, Howard J, Carlson K, Naleway SE. Biotemplating of a highly porous cellulose–silica composite from Apium graveolens by a low-toxicity sol–gel technique. JOM Jun. 2021;73(6):1736–44. https://doi.org/10.1007/s11837-021-04658-2.
[20] Ritz K, Young IM. Interactions between soil structure and fungi. Mycologist May 2004;18(2):52–9. https://doi.org/10.1017/S0269915X04002010.
[21] Harris K, Young IM, Gilligan CA, Otten W, Ritz K. Effect of bulk density on the spatial organisation of the fungus Rhizoctonia solani in soil. FEMS (Fed Eur Microbiol Soc) Microbiol Ecol May 2003;44(1):45–56. https://doi.org/10.1111/j.1574-6941.2003.tb01089.x.
[22] "Comparison of bulk densities for undisturbed soils and common urban conditions - Minnesota Stormwater Manual." https://stormwater.pca.state.mn.us/index.php/Comparison_of_bulk_densities_for_undisturbed_soils_and_common_urban_conditions(accessed Feb. 22, 2023).
[23] Ahmadi-Lahijani MJ, Farsi M. Evaluation of mycelium growth rate and yield of different isolates of edible white button mushroom (agaricus bispourus) in Iran. J Hortic Sci Jan. 2017;31:99–109.
[24] Bustillos J, Loganathan A, Agrawal R, Gonzalez BA, Gonzalez Perez M, Ramaswamy S, et al. Uncovering the mechanical, Thermal, and chemical characteristics of Biodegradable mushroom leather with Intrinsic Antifungal and antibacterial properties. ACS Appl Bio Mater May 2020;3(5):3145–56. https://doi.org/10.1021/acsabm.0c00164.
[25] Hoa HT, Wang C-L. The effects of Temperature and Nutritional conditions on mycelium growth of two oyster mushrooms (Pleurotus ostreatus and Pleurotus cystidiosus). MYCOBIOLOGY Mar. 2015;43(1):14–23. https://doi.org/10.5941/MYCO.2015.43.1.14.
[26] Ridley-Ellis D. Rate of growth. Centre for Wood Science & Technology; Apr. 15, 2016. accessed Feb. 15, 2023), https://blogs.napier.ac.uk/cwst/speed-of-growth/.
[27] Puettmann ME, Bergman R, Hubbard S, Johnson L, Lippke B, Oneil E, et al. Cradle-to-gate life-cycle inventory of US wood products production: CORRIM Phase I and Phase II products. Wood Fiber Sci 2010;42:15–28.
[28] Leiva FJ, Saenz-Díez JC, Martínez E, Jiménez E, Blanco J. Environmental impact of Agaricus bisporus mycelium production. Agric Syst Sep. 2015;138:38–45. https://doi.org/10.1016/j.agsy.2015.05.003.
[29] Abhijith R, Ashok A, Rejeesh CR. Sustainable packaging applications from mycelium to substitute polystyrene: a review. Mater Today Proc Jan. 2018;5(1):2139–45. https://doi.org/10.1016/j.matpr.2017.09.211. Part 2.
[30] Hadley PJ, Forbes AB, Rice BJ, Garnsworthy PC. Impact of the duration of control of cattle lice with eprinomectin on leather quality. Vet Rec 2005;157(26):841–4. https://doi.org/10.1136/vr.157.26.841.
[31] Li Z, Paudecerf D, Yang J. Mechanical behaviour of natural cow leather in tension. Acta Mech Solida Sin Feb. 2009;22(1):37–44. https://doi.org/10.1016/S0894-9166(09)60088-4.
[32] Janesch J, Jones M, Bacher M, Kontturi E, Bismarck A, Mautner A. Mushroom-derived chitosan-glucan nanopaper filters for the treatment of water. React Funct Polym Jan. 2020;146:104428. https://doi.org/10.1016/j.reactfunctpolym.2019.104428.
[33] Lee BU. Minimum sizes of respiratory particles carrying SARS-CoV-2 and the possibility of aerosol generation. Int J Environ Res Publ Health Sep. 2020;17(19):6960. https://doi.org/10.3390/ijerph17196960.
[34] WHO global air quality guidelines: particulate matter (PM2.5 and PM10), ozone, nitrogen dioxide, sulfur dioxide and carbon monoxide. In: WHO Guidelines Approved by the Guidelines Review Committee. Geneva: World Health Organization; 2021. Accessed: Feb. 14, 2023. [Online]. Available: http://www.ncbi.nlm.nih.gov/books/NBK574594/.
[35] Salvador P, Artíñano B, Alonso DG, Querol X, Alastuey A. Identification and characterisation of sources of PM10 in Madrid (Spain) by statistical methods. Atmos Environ Jan. 2004;38(3):435–47. https://doi.org/10.1016/j.atmosenv.2003.09.070.
[36] Font A, Baker T, Mudway IS, Purdie E, Dunster C, Fuller GW. Degradation in urban air quality from construction activity and increased traffic arising from a road widening scheme. Sci Total Environ Nov. 2014;497(498):123–32. https://doi.org/10.1016/j.scitotenv.2014.07.060.
[37] Hahnenberger M, Nicoll K. Meteorological characteristics of dust storm events in the eastern Great Basin of Utah, U.S.A. Atmospheric Environment Dec. 2012;60:601–12. https://doi.org/10.1016/j.atmosenv.2012.06.029.
[38] Aslannejad H, Hassanizadeh SM. Study of Hydraulic properties of Uncoated paper: image analysis and pore-scale modeling. Transport Porous Media 2017;120(1):67–81. https://doi.org/10.1007/s11242-017-0909-x.
[39] Du W, Iacoviello F, Fernandez T, Loureiro R, Brett DJL, Shearing PR. Microstructure analysis and image-based modelling of face masks for COVID-19 virus protection. Commun Mater Jun. 2021;2(1). https://doi.org/10.1038/s43246-021-00160-z. Art. no. 1.